

Bloch-Front Turbulence in a Periodically Forced Belousov-Zhabotinsky Reaction

Bradley Marts,¹ Aric Hagberg,² Ehud Meron,^{3,4} and Anna L. Lin¹

¹*Department of Physics, Duke University, Durham, North Carolina 27708, USA*

²*Mathematical Modeling and Analysis, Theoretical Division, Los Alamos National Laboratory, Los Alamos, New Mexico 87545, USA*

³*Department of Solar Energy and Environmental Physics, BIDR, Ben Gurion University, Sede Boker Campus 84990, Israel*

⁴*Department of Physics, Ben-Gurion University, Beer Sheva 84105, Israel*

(Received 20 April 2004; published 3 September 2004)

Experiments on a periodically forced Belousov-Zhabotinsky chemical reaction show front breakup into a state of spatiotemporal disorder involving continual events of spiral-vortex nucleation and destruction. Using the amplitude equation for forced oscillatory systems and the normal form equations for a curved front line, we identify the mechanism of front breakup and explain the experimental observations.

DOI: 10.1103/PhysRevLett.93.108305

PACS numbers: 82.40.Bj, 05.45.Xt, 47.20.Ky, 47.54.+r

Spatiotemporal disorder in extended systems commonly involves the spontaneous creation and annihilation of localized structures such as defects and vortices [1–3]. The driving forces for the nucleation of defects and vortices are instabilities of periodic patterns or fronts. Defects in periodic patterns often result from the Benjamin-Feir-Newell instability [4,5], while spiral-vortex nucleation in bistable systems has been related [6,7] to a front instability—the nonequilibrium Ising-Bloch (NIB) bifurcation [8–11].

The NIB bifurcation involves the destabilization of a stationary “Ising” front and the appearance of two counterpropagating “Bloch” fronts through a pitchfork bifurcation. It designates the onset of traveling wave phenomena and has been studied in several physical contexts including liquid crystals [12,13], chemical reactions [14], and catalytic surface reactions [15]. Theoretical studies of the NIB bifurcation have utilized the FitzHugh-Nagumo reaction-diffusion model and a variant of the complex Ginzburg-Landau equation that describes amplitude modulations of forced oscillations.

Studies of the FitzHugh-Nagumo model revealed the following scenario for spontaneous nucleation of vortices. In the vicinity of a NIB bifurcation, dynamic processes such as the increase of curvature along a front or interactions between fronts allow transitions between the two Bloch fronts [6,7,14]. A transition from one Bloch front to another represents a reversal in the direction of propagation. When the reversal occurs locally along a segment of the front line, a new pair of spiral vortices is nucleated at the points between the counterpropagating segments. Local curvature increases that lead to vortex nucleation can result from a transverse front instability [7]. This instability continues to drive vortex nucleation after nucleation events have already occurred and produces a state of spatiotemporal disorder.

Experimental indications pointing toward the relations among the NIB bifurcation, spontaneous vortex nucleation, and spatiotemporal disorder, can be found in studies

of chemical reactions [16] and liquid crystals [12,13,17]. However, direct experimental evidence tying front instabilities to vortex nucleation and disorder has not yet been provided. In this Letter we demonstrate experimentally how a transverse instability of a Bloch-front near the NIB bifurcation leads to vortex nucleation events, and how these events induce a transition to a disordered state we call “Bloch-front turbulence.”

The experimental system we study is the oscillatory photosensitive Belousov-Zhabotinsky (BZ) reaction, which is periodically forced in time with spatially uniform light. The chemical reaction occurs in a thin, porous-glass membrane 0.4 mm thick and 22 mm in diameter. The two faces of the membrane are fed by well-stirred reservoirs, each containing continuously refreshed reagents for the ruthenium-catalyzed BZ reaction [18,19]. Light from a low-intensity tungsten lamp is transmitted through the membrane and the optical density of the chemical concentration patterns is measured at 452 nm with a charge-coupled device camera.

The unforced reaction oscillates with a natural frequency f_0 and the chemical pattern is rotating spiral waves. We periodically forced the system with light at approximately twice the natural frequency ($f_f \sim 2f_0$) and with a varying amplitude I . When the forcing amplitude is large enough, the oscillations entrain to the forcing frequency in one of two phases that are π out of phase with each other. Depending on the initial state of the system, the oscillators may entrain in either of the two phases and patterns form in the membrane with fronts separating regions of different oscillation phase [20].

We prepare the initial state of the system with a pattern consisting of a single planar front separating the two different oscillation phases. This is achieved using a high forcing amplitude, $I = 67 \text{ W/m}^2$, and a forcing frequency near the natural oscillation frequency, $f_f = 0.025 \text{ Hz}$. Half of the reactor is forced π out of phase with the other half, creating a single stationary front in the center of the membrane. After the oscillations are entrained, the forc-

ing frequency is changed to near twice the natural frequency, $f_f = 0.06$ Hz, to lower amplitude, $I = 56$ W/m², and with a uniform spatial phase. The resulting pattern is a standing wave with a single nearly planar front between two phases, as shown in Fig. 1(a) [21].

At the forcing amplitude $I = 56$ W/m² the front is stationary (Ising front). It begins to travel when the forcing amplitude is reduced past a critical intensity $I \sim 26$ W/m². Further reduction in the forcing amplitude produces traveling fronts (Bloch fronts) with larger front velocities, indicating the presence of a NIB bifurcation near $I = 26$ W/m².

Near the NIB bifurcation we also observe the transverse instability of the Bloch front. As shown in Figs. 1(a)–1(c) the transverse instability of the Bloch front causes small perturbations of a nearly planar front to grow. As the perturbations grow they cause the nucleation of spiral-vortex pairs. Figures 1(d)–1(f) show the spatial vortex distribution; the vortices are first distributed along the initial front line, but as time evolves they

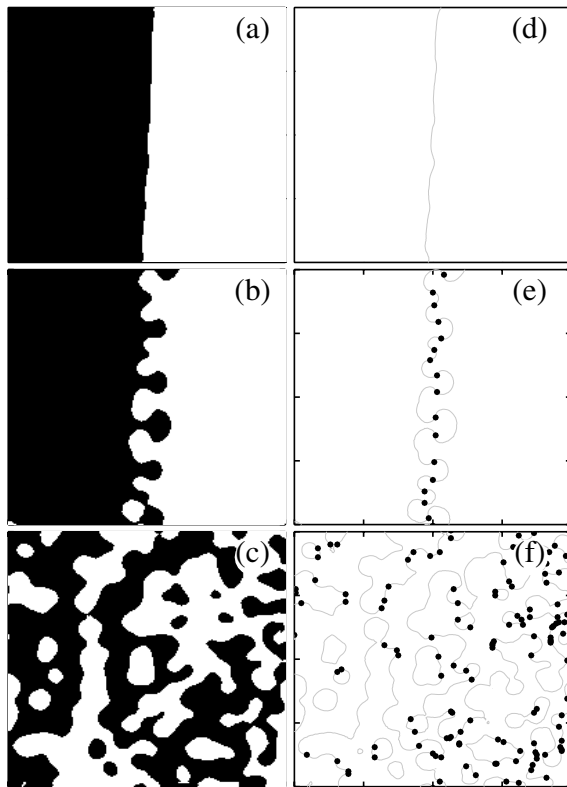


FIG. 1. Spiral-vortex nucleation in the BZ system. Frames (a)–(c) show the phase of the oscillations at near half the driving frequency for three different times ($t = 100, 300$, and 1700 s) [21]. Frames (d)–(f) show the position of the vortices along the front line (as solid circles) at the corresponding times. (a) The initial nearly planar front is unstable to transverse perturbations. (b) Vortices form in pairs along the front line. (c) Vortices eventually fill up the entire system. The figures show a 19.1 mm \times 19.1 mm (200×200 pixel) region of the BZ system with $I = 25$ W/m², $f_f = 0.06$ Hz. Chemical conditions are given in Ref. [19].

108305-2

fill up the whole system into a state of Bloch-front turbulence.

New vortex pairs are continually created and the number of vortices grows in time as Fig. 2 shows. After the initial transient an asymptotic mean value of about 90 is reached. Fluctuations around the mean are caused by the creation and destruction of vortex pairs. We also observe vortices meandering in and out of the 19.1×19.1 mm² region shown in Fig. 1. However, this occurs far less often than pairs of spiral vortices are created and destroyed, and so does not significantly contribute to the vortex fluctuations.

The experimental system can be modeled by a variant of the complex Ginzburg-Landau (CGL) equation which describes amplitude modulations of a periodically forced oscillatory system near a Hopf bifurcation to uniform oscillations. The equation for the oscillation amplitude is [22]

$$\partial_t A = (\mu + i\nu)A + (1 + i\alpha)\nabla^2 A - (1 + i\beta)|A|^2 A + \gamma A^* \quad (1)$$

where μ is the distance from the Hopf bifurcation, ν is the detuning, α is dispersion, β is a nonlinear frequency correction, and γ is the forcing amplitude. Equation (1) has two stable stationary solutions which correspond to uniform oscillations at exactly half the forcing frequency. The oscillation phases of the two solutions differ by π with respect to one another. Equation (1) also has stationary Ising front solutions biasymptotic to the two stationary uniform solutions. These front solutions lose stability to Bloch fronts as γ is decreased below the NIB bifurcation, $\gamma_{\text{nib}}(\nu)$ [9]. The front solutions can also go through a transverse instability as γ is decreased below another threshold, $\gamma_T(\nu)$ [23].

Numerical solutions of Eq. (1) in the vicinity of the NIB bifurcation reproduce the experimental observa-

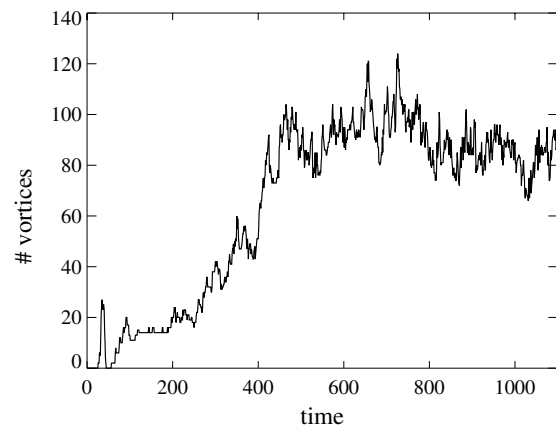


FIG. 2. The total number of vortices in a 19.1 mm \times 19.1 mm (200×200 pixel) region of the BZ system. Over time the number of vortices increases from the initial front state with zero until the spirals fill the entire system and the total number of vortices fluctuates around a mean value of about 90.

108305-2

tions, as Fig. 3 shows. As in the chemical experiment, the initial nearly planar front [Figs. 3(a) and 3(d)] is unstable to transverse perturbations and small perturbations grow and nucleate vortex pairs [Figs. 3(b) and 3(e)]. The resulting state shown in Figs. 3(c) and 3(f) is Bloch-front turbulence with the continual creation and destruction of vortex pairs.

A closer examination of a vortex nucleation event can be obtained from the normal form equations for a curved front line in the vicinity of the NIB bifurcation. The equations for the front curvature, κ , and the planar front velocity, C_0 , are [24]

$$\frac{d\kappa}{dt} = -\left(\kappa^2 + \frac{\partial^2}{\partial s^2}\right)C_n, \quad (2a)$$

$$\frac{dC_0}{dt} = (a_{\text{nib}} - a)C_0 - bC_0^3 + c\kappa + \frac{\partial^2 C_0}{\partial s^2}, \quad (2b)$$

where C_n , the normal front velocity, is related to κ and C_0 through the relation $C_n = C_0 - D\kappa$, s is arclength, and $\frac{d}{dt}$ is the total time derivative: $\frac{d}{dt} = \frac{\partial}{\partial t} + \frac{ds}{dt} \frac{\partial}{\partial s}$. The arclength

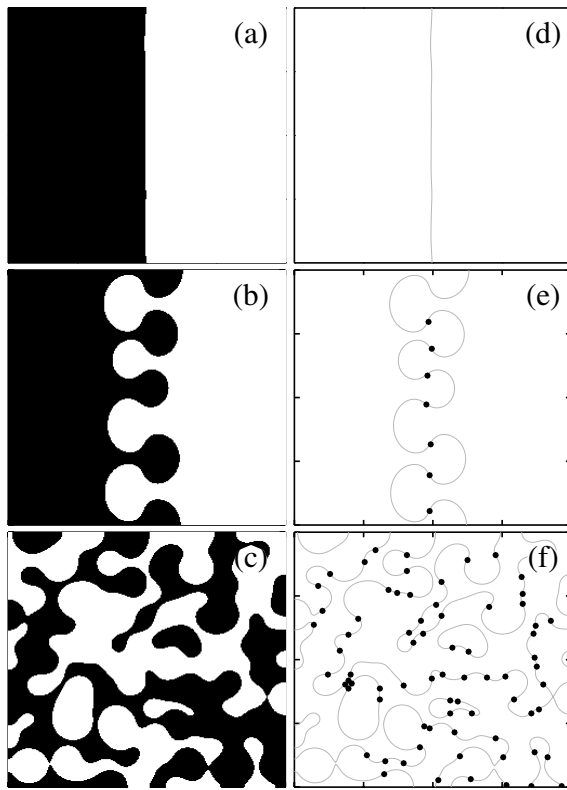


FIG. 3. Spiral-vortex nucleation and formation of Bloch-front turbulence in a numerical solution of the CGL Eq. (1). Frames (a)–(c) show the phase $\arg(A)$ of the solution at three different times, $t = 0, 620, 7820$. Perturbations on the unstable front solution grow and pairs of vortices form along the front. Frames (d)–(f) show the front line [defined as $(A) = 0$] and vortices [$(A) = (A) = 0$] (solid circles) at the corresponding times. The parameters are $\mu = 0.5$, $\nu = 0.15$, $\alpha = 0.35$, $\beta = 0$, $\gamma = 0.2$ on a domain size of $[x, y] = [256, 256]$ with no-flux boundary conditions.

changes in time, when the front is curved and moving, according to $\frac{ds}{dt} = \int_0^s \kappa C_n ds'$.

Equations (2) capture the NIB bifurcation for a planar front as the bifurcation parameter a crosses the threshold a_{nib} ; an Ising front solution, $(C_0, \kappa) = (0, 0)$, loses stability and two stable Bloch-front solutions, $(C_0, \kappa) = [\pm\sqrt{(a_{\text{nib}} - a)/b}, 0]$, appear. In the Bloch regime ($a < a_{\text{nib}}$) Eqs. (2) have a kink solution bi-asymptotic (as $|s| \rightarrow \infty$) to the two Bloch-front solutions as Fig. 4(a) shows. In the two-dimensional x - y plane this kink solution describes a rotating spiral wave [Fig. 4(b)].

Equations (2) also imply that Bloch fronts close to the NIB bifurcation are unstable to transverse perturbations provided $c/D > 0$ [25]. To see this, we study the stability of planar Bloch fronts to perturbations of the form $(\delta C_0, \delta\kappa) \exp(\sigma t + iQs) + \text{c.c.}$. Inserting the perturbed forms for C_0 and κ in Eqs. (2) gives the neutral stability ($\sigma = 0$) relation

$$a_{\text{tr}}(Q) = a_{\text{nib}} - \frac{c}{2D} + Q^2. \quad (3)$$

The first mode to grow is the zero mode, $Q = 0$. Within the range $a_{\text{nib}} - \frac{c}{2D} < a < a_{\text{nib}}$ Bloch fronts are unstable to transverse perturbations. As a approaches the NIB bifurcation threshold, a_{nib} , modes with higher and higher wave numbers grow. When the curvature perturbations produced by these modes are sufficiently large, local transitions between the two Bloch fronts are induced and vortex nucleation events take place [26] as demonstrated in Fig. 5.

In conclusion, we have demonstrated, in a periodically forced oscillatory Belousov-Zhabotinsky reaction, a mechanism for creating spatiotemporal disorder. The mechanism consists of the creation of spiral-vortex pairs through a transverse instability of fronts in the vicinity of a nonequilibrium Ising-Bloch bifurcation. We used an amplitude equation model, the forced complex Ginzburg-

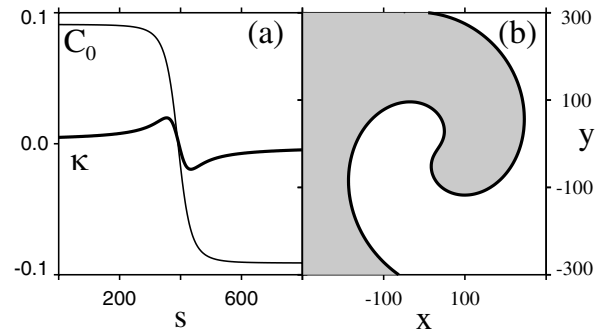


FIG. 4. Spiral wave solution of the front line Eqs. (2). (a) The front velocity and curvature have a kink solution bi-asymptotic to the two block fronts as $|s| \rightarrow \infty$. (b) In the x - y (laboratory) coordinate frame the kink solution is a spiral wave. The core of the spiral wave is characterized by zero curvature and front velocity. Parameters: $a = 5.99$, $a_{\text{nib}} = 6.0$, $b = 0.17$, $c = 6.0$, $D = 1.0$.

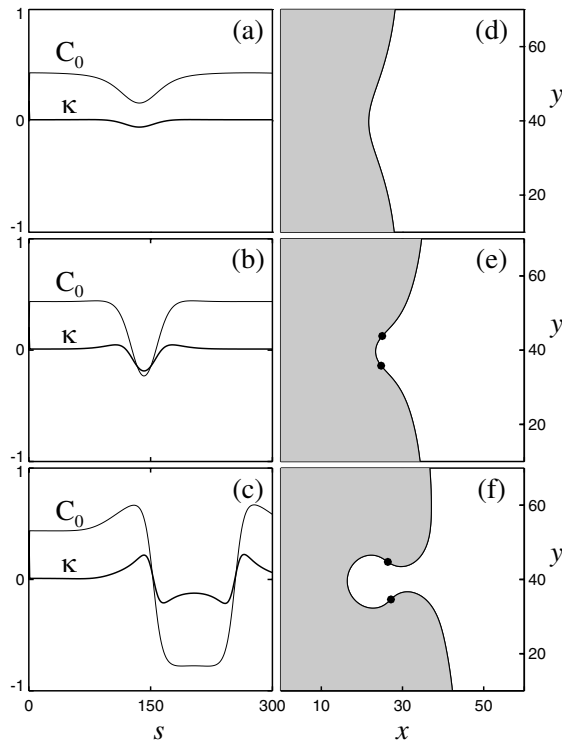


FIG. 5. Nucleation of a spiral-vortex pair in the front line equations (2). (a)–(c) The front velocity C_0 and curvature κ vs the arclength s . (d)–(f) The corresponding representation in the $x - y$ (laboratory) coordinate frame. (a),(d) A small perturbation in the curvature grows. (b),(e) A portion of the domain reverses direction and a spiral-vortex pair nucleates along the front line. (c),(f) A pair of rotating spiral waves forms. Parameters: $a = 5.97$, $a_{\text{nib}} = 6.0$, $b = 0.165$, $c = 6.03$, $D = 1.0$.

Landau equation, to reproduce the experimental observations with numerical solutions, and further described the mechanism for vortex creation with the normal form equations for a curved front line.

This work was supported by the U.S.-Israel Binational Science Foundation (Grant No. 9800129), the Department of Energy under Contract No. W-7405-ENG-36, and the DOE Office of Science Advanced Computing Research program in Applied Mathematical Sciences.

[1] P. Couillet, L. Gil, and J. Lega, *Phys. Rev. Lett.* **62**, 1619 (1989).
 [2] S.W. Morris, E. Bodenschatz, D.S. Cannell, and G. Ahlers, *Phys. Rev. Lett.* **71**, 2026 (1993).
 [3] A.L. Porta and C.M. Surko, *Phys. Rev. E* **56**, 5351 (1997).
 [4] A.C. Newell, in *Lectures in Applied Mathematics* (American Mathematical Society, Providence, RI, 1974), Vol. 15, p. 157.
 [5] I.S. Aranson and L. Kramer, *Rev. Mod. Phys.* **74**, 99 (2002).
 [6] A. Hagberg and E. Meron, *Phys. Rev. Lett.* **72**, 2494 (1994).

[7] A. Hagberg and E. Meron, *Chaos* **4**, 477 (1994).
 [8] H. Ikeda, M. Mimura, and Y. Nishiura, *Nonlinear Anal. Theory Methods Appl.* **13**, 507 (1989).
 [9] P. Couillet, J. Lega, B. Houchmanzadeh, and J. Lajzerowicz, *Phys. Rev. Lett.* **65**, 1352 (1990).
 [10] M. Bode, A. Reuter, R. Schmeling, and H.-G. Purwins, *Phys. Lett. A* **185**, 70 (1994).
 [11] A. Hagberg and E. Meron, *Nonlinearity* **7**, 805 (1994).
 [12] S. Nasuno, N. Yoshino, and S. Kai, *Phys. Rev. E* **51**, 1598 (1995).
 [13] T. Frisch and J.M. Gilli, *J. Phys. II (France)* **5**, 561 (1995).
 [14] D. Haim, G. Li, Q. Ouyang, W.D. McCormick, H.L. Swinney, A. Hagberg, and E. Meron, *Phys. Rev. Lett.* **77**, 190 (1996).
 [15] G. Haas, M. Bär, I.G. Kevrekidis, P.B. Rasmussen, H.-H. Rotermund, and G. Ertl, *Phys. Rev. Lett.* **75**, 3560 (1995).
 [16] K.J. Lee and H.L. Swinney, *Phys. Rev. E* **51**, 1899 (1995).
 [17] T. Kawagishi, T. Mizuguchi, and M. Sano, *Phys. Rev. Lett.* **75**, 3768 (1995).
 [18] Diagrams of the reactor are presented in Fig. 2 of Q. Ouyang and H.L. Swinney, *Chaos* **1**, 411 (1991); also see Fig. 1 of Q. Ouyang, R. Li, G. Li, and H.L. Swinney, *J. Chem. Phys.* **102**, 2551 (1995).
 [19] The chemical concentrations in the two chemical reservoirs separated by the porous membrane were, reservoir I: 0.22 M malonic acid, 0.184 M potassium bromate, 0.8 M sulfuric acid; reservoir II: 0.184 M potassium bromate, 1×10^{-3} M Tris(2,2'-bipyridyl)dichlororuthenium(II)hexahydrate, 0.8 M sulfuric acid. Each reservoir volume is 8.3 ml and the flow rate of chemicals through reservoir I was 20 ml/hr while through reservoir II it was 5 ml/hr. Chemicals were premixed before entering each reservoir; a 10 ml premixer and a 0.5 ml premixer fed reservoirs I and II, respectively. The experiments were conducted at room temperature.
 [20] A.L. Lin, M. Bertram, K. Martinez, H.L. Swinney, A. Ardelea, and G.F. Carey, *Phys. Rev. Lett.* **84**, 4240 (2000).
 [21] The image data recorded by the camera is processed by frequency filtering with a bandpass filter centered at $f_f/2 = 0.03$ Hz with a width of 0.012 Hz. We treat the resulting signal as $u = ae^{if_f t/2}$ and plot the phase of the complex amplitude a . The front line is defined as $\text{Re}(a) = 0$ and the vortex positions are $\text{Re}(a) = \text{Im}(a) = 0$.
 [22] J.M. Gambaudo, *J. Diff. Eq.* **57**, 172 (1985); supplementary material is available at <http://math.lanl.gov/BlochFront/>
 [23] A. Yochelis, C. Elphick, A. Hagberg, and E. Meron, Report No. LA-UR-03-5938 [Physica D (Amsterdam) (to be published)].
 [24] A. Hagberg and E. Meron, *Phys. Rev. Lett.* **78**, 1166 (1997).
 [25] Since we do not know how the parameters of Eq. (1) are related to the oscillatory BZ reaction we cannot determine the sign of c/D . The sign, however, is expected to be positive if for $a > a_{\text{nib}}$ the Ising front is unstable to transverse perturbations.
 [26] A. Hagberg and E. Meron, *Physica (Amsterdam)* **123D**, 460 (1998).